

Combined Simulated annealing and Improved Binary PSO based Optimal Corona Ring Design for High Voltage Transmission Line

Abstract. Electric stress is caused by the high field in the metal flange at the end. Corona and surface electrical discharges will be triggered, which may cause early deterioration. Under extreme circumstances, a total insulation flash over will happen. Both internal and external discharge activities are taken into consideration while constructing the ideal insulator in typical conditions. When the insulator is subjected to high voltage there will be an uneven electric field distribution occurs. This will reduce the reliability of the insulator and ageing occurs. It will leads to damage of insulator and replacement of insulator. To protect insulator from heavier damage due to uneven electric field is negated by using corona ring in high voltage transmission line. Corona ring makes the uneven electric field distribution into uniform electric field hence the damage of insulator is avoided. This paper demonstrates how to evaluate the electric field and voltage distribution along composite insulators for system voltages ranging from 765 kV ac using software packages based on the idea of numerical analysis technique. This work uses ANSYS Maxwell to compute the electric field distribution in high voltage and low voltage terminals for different diameters at varying heights, both with and without a corona ring. ANSYS is used to calculate mechanical strength of insulator. The structural analysis, stress analysis and thermal analysis carried out to check the withstanding capability of insulator during heavy force, heavy stress and high temperature. The main objective is to reduce the maximum Electric field distribution of the along 220 kV. The optimization is carried out by through the use of Combined Simulated Annealing and Improved Binary Particle Swarm Optimization (CSAIBPSO).

Streszczenie. Naprężenia elektryczne są spowodowane wysokim polem w metalowym kołnierzu na końcu. Wystąpią wyładowania koronowe i powierzchniowe, które mogą spowodować przedwczesne zniszczenie. W ekstremalnych okolicznościach nastąpi całkowite przeskok izolacji. Przy konstruowaniu idealnego izolatora w typowych warunkach brane są pod uwagę zarówno wewnętrzne, jak i zewnętrzne działania związane z wyładowaniami. Gdy izolator zostanie poddany działaniu wysokiego napięcia, nastąpi nierównomierny rozkład pola elektrycznego. Zmniejszy to niezawodność izolatora i nastąpi starzenie się. Doprowadzi to do uszkodzenia izolatora i wymiany izolatora. Aby chronić izolator przed większymi uszkodzeniami spowodowanymi nierównomiernym polem elektrycznym, zanegowano użycie pierścienia koronowego w linii przesyłowej wysokiego napięcia. Pierścień koronowy powoduje nierównomierny rozkład pola elektrycznego na jednolite pole elektryczne, dzięki czemu unika się uszkodzenia izolatora. W artykule przedstawiono sposób oceny pola elektrycznego i rozkładu napięcia wzdłuż izolatorów kompozytowych dla napięć systemowych w zakresie od 765 kV prądu przemiennego przy użyciu pakietów oprogramowania opartych na idei techniki analizy numerycznej. W tej pracy wykorzystano ANSYS Maxwell do obliczenia rozkładu pola elektrycznego w zaciskach wysokiego i niskiego napięcia dla różnych średnic i różnych wysokości, zarówno z pierścieniem koronowym, jak i bez niego. ANSYS służy do obliczania wytrzymałości mechanicznej izolatora. Analiza strukturalna, analiza naprężeń i analiza termiczna przeprowadzana w celu sprawdzenia wytrzymałości izolatora podczas dużych sił, dużych naprężeń i wysokiej temperatury. Głównym celem jest zmniejszenie maksymalnego rozkładu pola elektrycznego wzdłuż 220 kV. Optymalizację przeprowadza się poprzez zastosowanie połączonego symulowanego wyżarzania i ulepszonej optymalizacji roju cząstek binarnych (CSAIBPSO). (Połączone symulowane wyżarzanie i udoskonalona optymalna konstrukcja pierścienia koronowego oparta na binarnym PSO dla linii przesyłowej wysokiego napięcia)

Keywords: Insulator, High voltage transmission line, MAXWELL, Combined Simulated Annealing and Improved Binary Particle Swarm Optimization

Słowa kluczowe: Izolator, linia przesyłowa wysokiego napięcia, MAXWELL, połączone symulowane wyżarzanie i ulepszona optymalizacja roju cząstek binarnych.

1.Introduction

Extra high voltage power lines have been a common means of transferring electricity from power plants to final consumers in recent years. The insulators must endure a variety of environmental pressures, including rain, snow, and pollution, R. S. Gorur et al. [1] discussed about the development of non-ceramic (polymeric) insulators which will replace the porcelain and glass insulator for outdoor application of High Voltage (HV) network. Hartings [2] et al. elaborated the electric field distribution along composite and ceramic insulators during pollution tests. Chakravorti et al. [3] developed an algorithm based for calculating the power frequency and impulse electric field distributions around a HV insulator either with uniform or non-uniform surface pollution.

Vaillancourt et al. [4] have done the some adjustments to redesign composite insulators. Chen et al. [5] used the electric field mapping method to detect conductive internal defects of a 110 kV composite insulator. Gela et al. [6] initiated a research work to analyze the performance of non-ceramic insulators from the live line working viewpoint. Feng Huo et al. [7] outlined the finite element approach used to determine the electric field distribution of a 750 kV transmission line on six cross-arm towers. Grading ring geometry factors can help generate a more uniform electric field and voltage distribution, as addressed by Nadjim Alti Abdelhafid et al. [8]. Benalia m'hamdi et al. [9] explained to

reduce the corona ring on a 400 kV AC transmission line composite insulator in order to enhance the distributions of the electric field and potential.

In order to improve the electric field and potential distributions and thereby reduce corona discharges on 230 kV AC transmission line composite insulator, Shiling Zhang et al. [10] used corona rings at the HV end fitting. A modified PSO algorithm is used to minimize the objective function in order to solve the optimization problem. The corona ring structure is further enhanced by B. M'hamdi et al. [11] who created a three-dimensional model. They also carried out an E-field calculation using Finite Element Method (FEM) software.

S. Chakravorti, et al. [13] have done Boundary-Element research on the Electric Field and shape of insulators around HV Insulators with or without Pollution. S.K.B.Pradeep Kumar[14] et al. detailed about the best way to infuse and grade combined DGs and capacitor banks to minimize line loss and boost voltage in radial circuit systems.. T. Zhao [15] et al. explained about calculating the potential distribution and electric field along non-ceramic insulators while taking transmission tower and conductor effects into account. E. A. Cherney, [16] et al. outlined about non-ceramic insulators: a straightforward design that needs careful consideration.

H.El-Kishky, [17] et al. described about energy computation and Electric field on wet insulating surfaces. G.

H. Vaillancourt, [18] et al. analyzed about the electric field measurement method to detect defective composite insulators on high-voltage power lines. G. Gela [19], et al. examined the methodology for evaluating composite insulator Electrical and mechanical integrity before live working condition.

. Vaillancourt,[20] et al. demonstrated about the porcelain suspension insulators on high-voltage power lines with the new live line tester. Benalia M'hamdi [25] et al. have utilized meta-heuristic algorithm to obtain optimal values and electric field distribution by minimizing corona ring in 400 kV AC transmission line. From the survey of literature there is a need to algorithm to optimize Electric field distribution.

Existing problems

An HV insulator needs to be able to tolerate mechanical and electrical stress. Among these, electrical stress is a crucial consideration for both regular operations and the transient situations brought on by switching activities and lightning. Fig.1.shows the flowchart for the proposed system design using Finite Element Analysis(FEA).

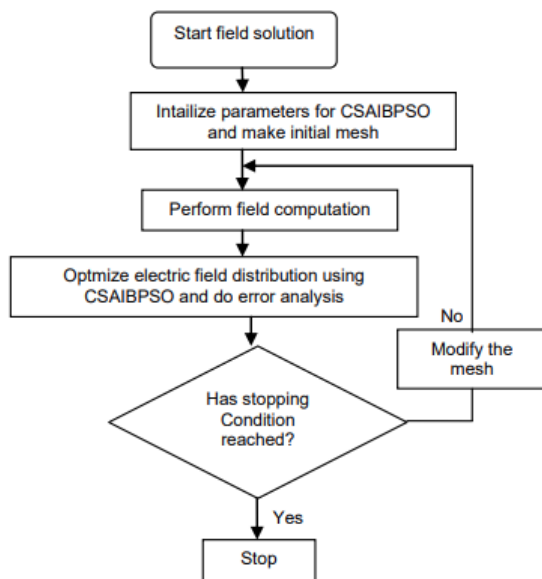


Fig.1.Flowchart for the proposed system design using FEA

The knowledge of the relationship between the contact angle, size, shape and distribution of water droplets on the non-ceramic insulator surface and the electric field strength enhancement around the surface of water droplets is still rather limited. The flashover usually happens during fog and light rain conditions.

Proposed methodology

The foremost goal of this paper is to study the electric field and voltage distribution along composite insulators under normal conditions. Commercially available software ANSOFT MAXWELL based on the FEM is employed for the modelling and the calculation for the composite insulators under normal conditions. The precise objectives and the main contributions of the paper can be summarized as follows: Develop the model of a composite insulator using ANSOFT Software.

The geometry and dimensions of typical composite insulators have been used for modeling purposes. To develop the models of typical 765Kv of composite insulators have been used.

The field distribution along the length of the composite insulators characterizes their electrical performance. Since the metal end fitting is one of the main characteristics of a composite insulator, by improving one and comparing the

results, it is possible to determine which performs better under various conditions.

The primary goal of this work is to improve the insulator's long-term performance. We have used shapes of corona rings are circle and ellipse which are tested under different conditions. CSAIBPSO algorithm is utilized in the proposed method to minimize the maximum Electric field distribution.

Flashover caused due contamination

Due to its hydrophobic properties, polymer material prevents water from adhering to its surface. Rather than covering the entire surface, water condenses into tiny droplets. This suggests improved performance by lowering the leakage current and the likelihood of dry band formation.

Design of composite insulator

The two primary tasks of this section are:

- To determine which simplification models of composite insulators can be used to study the EFVD along the insulators with different design a metal end fitting.
- To investigate some basic features related to the electric field enhancement by using grading material, corona ring.

Composite insulator model

For a 765 kV composite insulator, a lot more elements are needed than for a 34.5 kV composite insulator in order to obtain correct results. The EFVD along composite insulators can be calculated using the boundary element approach. Certain reductions in the complexity of the composite insulator model are required to minimize the computation time when examining long insulators.

Simplified composite insulator dimensions and geometry are displayed in Fig. 2. To determine which insulator component may be simplified with the least impact on the EFVD along the composite insulators.

Metal fittings are installed on the insulator at both the line and ground ends. Fiberglass reinforced polymer rod has a relative permittivity of 7.2 and silicone rubber has a permittivity of 4.3, which together form the insulator. The air surrounding the insulator has a relative permittivity of 1.0. The parameter values are given in cm.

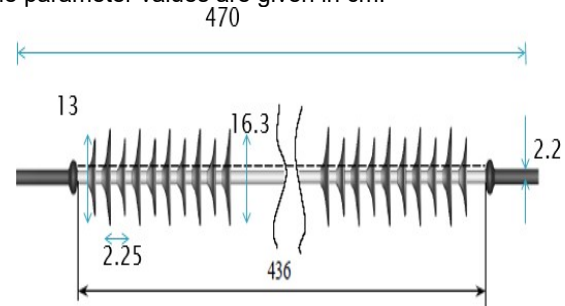


Fig.2.Simplified geometry and dimensions of the composite insulators

Structure and materials

Fiber Reinforced Plastic (FRP) is the common material used in composite insulators, on which end fittings are fastened. The insulator must be covered with a polymer known as housing in order to shield the core from external forces. Epoxies were widely utilized for this purpose at first, but hydrocarbons and silicones have since taken over due to considerable discomfort. Table 1 shows the design parameters.

Silicone rubber was primarily utilized as a composite insulator in outdoor high-voltage network applications. since silicone rubber resists UV rays and heat produced by dry band arcing better than Ethylene Propylene Dien Monomer (EPDM).The structure is divided into three subdomains: the silicone rubber insulation material, the fiber-reinforced

plastic core domain situated in the middle of the insulation, and the metal fitting placed at the ends of the insulator, which is made of forged steel.

Table 1. Design parameters[12,27]

S.No	Design parameters	Values [cm]
1.	Insulator distance	470
2.	Core Length (FRP)	350
3.	Creepage Distance	436
4.	Core Thickness	16
5.	Polymer material sheath Thickness	22
6.	Metal end fitting distance	154
7.	Polymer material weather sheds Distance	2.25
8.	Polymer material weather sheds Thickness	16.3,13

Table 2. shows Basic Insulation Level (BIL) and Specified Mechanical Load(SML) levels of insulator. In this paper, forged steel is used to give mechanical support to insulator. Silicon rubber is used to give flexibility to insulator. Two end of the insulator are made up of conductive medium. Aluminium is used as a conductive medium.

Table 2. BIL and SML levels of insulator

Voltage rating(Kv)	BIL(Kv)	SML [KN]
345	1425	No
500	2250	No
765	2700	Yes
1000	3200	Yes

Table 3 shows the for particular voltage correct value of force to be applied. For 345kv BIL is 1425 and SML is 100-210. Here we have applied the voltage of 765kv for this BIL is 2700 and SML is 100-400. We have chosen 160KN force.

Table 3. Corona ring

Voltage rating(Kv)	Corona ring added	
	Line end	Grounded end
138	No	No
230	Yes	No
345	Yes	Yes
500	Yes	Yes
765	Yes	Yes
1000	Yes	Yes
1200	Yes	Yes

Model of corona ring

The insulator is damaged when the electric field is at its strongest on the HV side. Corona rings are utilized along the two insulator terminals to lessen the electric field and make it more consistent. The metal used to design the corona ring is Aluminium. The economical shapes of corona ring we used are circle and ellipse. In this shapes electric field distribution is uniform and reduced.

Grading rings parameters optimization based on CSAIBPSO.

In computational intelligence method, PSO algorithm is the iterative procedure to obtain optimal solution[13-14]. It searches solution from the population of particles. BPSO works on discrete space. Research has shown that PSO and BPSO are not converged properly. One limitation with using BPSO to solve a binary solution problem is that a non-standard method equation is used to calculate the particle's position with a random number 0 or 1. New positions in the swarm for a selected individual can be signified as Equation (1)-(2)

$$(1) \quad v_{ij}^{k+1} = w_1 \otimes (pbest_{ij}^k \oplus x_{ij}^k) + w_2 \otimes (gbest_{ij}^k \oplus x_{ij}^k)$$

$$(2) \quad x_{ij}^{k+1} = x_{ij}^k \oplus v_{ij}^{k+1}$$

where $v_{ij}^{(k+1)}$ is the updated velocity of j^{th} dimension in i^{th} particle at iteration $k+1$, $x_{ij}^{(k+1)}$ is the updated current position of the j^{th} dimension in i^{th} particle at iteration $k+1$. $pbest_{ij}^k$ is the particle best of individual j^{th} dimension in i^{th} particle at iteration k , $gbest_{ij}^k$ is the global best of individual j^{th} dimension in i^{th} particle at iteration k , \otimes is AND operator, \oplus is XOR operator, $+$ is OR operator and w_1 and w_2 are two random binary integer numbers between $[0,1]$ [22-23].

Very Fast SA

The idea of annealing melted metals over is replicated by simulated annealing. If the initial temperature is high in SA it will take more convergence time to find the optimal solution. Hence Gaussian or Boltzmann function is incorporated in the traditional SA i.e Very Fast SA Generative functions is given in Equation (3)-(4) to increase the speed of convergence [12].

$$(3) \quad g(X) = (2\pi T)^{-D/2} e^{-(X^2/2T)}$$

where D - dimension of the search space and ΔX - the rate of change of X .

$$(4) \quad X = X_0 + \Delta X$$

where X_0 denotes the current state and X shows the next state of variables'. The temperature in the k^{th} stage of the algorithm is calculated by Equation(5):

$$(5) \quad T_k = T_0 / \ln K$$

Cauchy distribution in Fast SA, is given in Equation. (6)

$$(6) \quad g(X) = T / \Delta X^2 + T^2)^{(D+1)/2}$$

Decrease in the temperature in the FSA is given in Equation (7)

$$(7) \quad T_k = T_0 / K$$

Since there isn't a fast approach to produce random numbers for high-dimensional issues, the issue with this algorithm is trying to obtain a random number for ΔX that mimics the Cauchy distribution. Annealing is computed in Very Fast SA (VFSA) using Equation. (8)

$$(8) \quad T_i(k) = T_0 e^{-c_i k^{1/D}}, i = 1, 2, 3, \dots, D$$

$i - j^{th}$ variable of the cost function, C_i is a constant that can have different values depending on the problem. It is obvious that annealing follows exponential function [21]. Reduction of maximum E-field distribution is the primary objective of the proposed method. In the objective function, maximum electric field strength and grading ring structure parameters.

In this paper, the optimization process is based on CSAIBPSO algorithm. One such formulation for the optimization issue is as stated in Equation (9).

$$(9) \quad f(x1, x2, x3) = E(H, R, T)$$

where $x1, x2, x3$ corresponds to H, R and T respectively.

E - E-field [kV/cm].

H -grading ring position from HV electrode [mm].

R -grading ring radius [mm].

T - the thickness of the grading ring tube [mm].

Results and Discussion

The findings of the simulation work for an insulator with a 765 kV ring are provided in this section. Here, the distribution of the electric field at low voltage and high voltage terminals for an insulator with and without a corona ring of different diameters and heights is estimated. Next, the insulator's electric field distribution in wet, dry, polluted, and water droplet conditions is evaluated. Then the results of structural deformation, stress analysis and thermal analysis are analyzed.

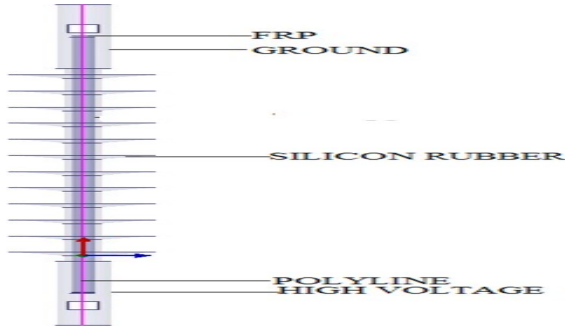


Fig 3. 3D Insulator Modelling

Figure 3 displays the 3D modeling. In this section, the electric field estimates for all voltage ratings are shown in a dry environment without taking any corona mitigation techniques into account. Beginning 1 mm from the energized end fitting and ending at the grounded end fitting, the electric field is computed in a straight line. As advised by Electric Power Research Institute (EPRI), the measurement line is made sure to be straight and to be 1 mm above the composite insulator's surface.

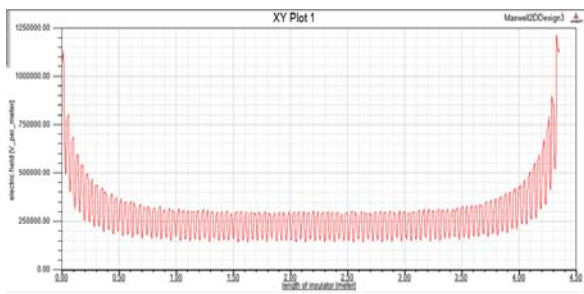


Fig.4.Electric field distribution under dry condition

Without the use of a corona ring, the electric field distribution in the insulator is depicted in Figure. 4. In this condition uneven electric field breaks the whole part of the insulator. The maximum peak voltage observed from the graph is 1.2kv/mm.

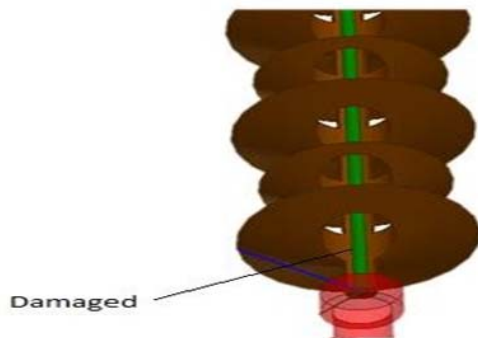


Fig 5. Damaged Insulator

Damaged Insulator

When there is no wind, the highest electric field value along the composite insulators' surface is shown in Figure.5 as a field value at the metallic energized rail's triple point is air. At higher voltages, the electric field stress along composite insulators is still higher even if the dry arc distance, which is used to calculate the electric field, increases with the system voltage. The threshold for corona initiation is defined as 1.2 kV/mm. According to the findings, a corona mitigation 230 kV and higher is necessary.

When comparing composite insulators to porcelain, it was discovered that the maximum electric field values for situations under 500 kV were comparatively higher. Additionally, compared to porcelain, composite insulators are more vulnerable to damage from corona. Therefore, even at system voltages lower than 500 kV, mitigation devices such as corona rings are strongly advised at the energized high voltage end.

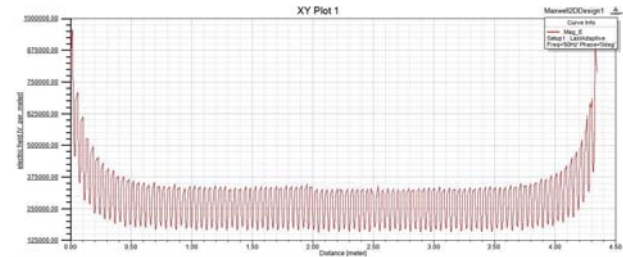


Fig 6. Electric field distribution of Damaged Insulator

Figure.7 and Figure.8. are the simulation result of insulator damaged and without damage. It is therefore strongly advised to use mitigation devices such as corona rings at the energized high voltage end, even for system voltages lower than 765 kV.

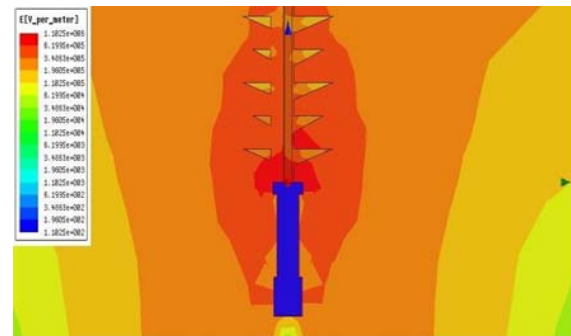


Fig 7. Electric field distribution damaged

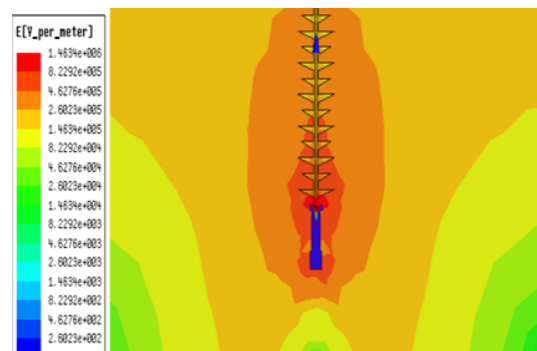


Fig 8 Electric field insulator distribution Insulator

Variation of diameter and height at high voltage

From the Figure 9, it discussed about the variation in diameter of the ring with respect to the change in height of the ring at insulator at the high voltage terminal. Using a corona ring in an insulator not only makes the electric field more uniform but also lessens it as compared to not using one. In order to make the ring performance more efficient we increased the ring diameter to certain value. The electric field reaches its maximum of 0.49 kV/mm at a height of 120 mm in a 300 mm diameter.

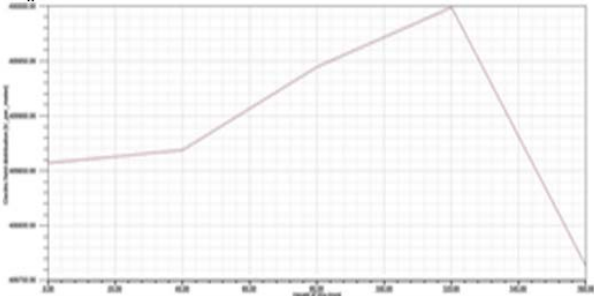


Fig: 9 Diameter-300 mm

We fixed the diameter of ring at 400mm. It is shown in Figure. 10. When compared to 300mm there is reduced electric field distribution in 400mm ring. In 400mm ring the reduced electric field is achieved in 120mm height at high voltage side. At height of 120mm, the electric field distribution is 0.48kv/mm. Hence the increase in diameter decreases the electric field distribution.

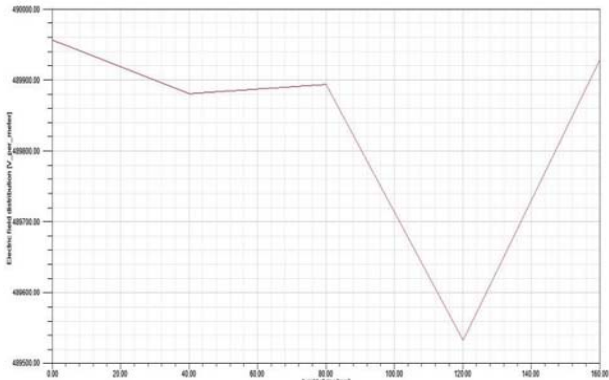


Fig.10. Diameter-400 mm

Then we fixed the diameter of ring at 500mm. When compared to 400mm there is reduced electric field distribution in 500mm ring. It is shown in Figure 11. In 500mm ring the reduced electric field is achieved in 80mm height at high voltage side. At height of 80mm, the electric field distribution is 0.48kv/mm. Maximum electric field at the height of 160mm is 0.489kv/mm

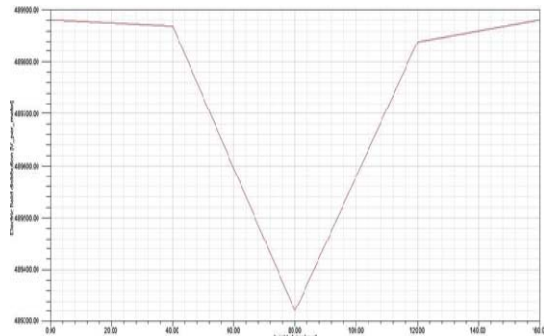


Fig: 11. Diameter-500 mm

Then the diameter is modified for a ring at 600mm. When compared to 500mm there is reduced electric field distribution in 600mm ring. In 600mm ring the reduced electric field is achieved in 40mm height at high voltage side. At height of 40mm, the electric field distribution is 0.4kv/mm. At 80 mm in height, the maximum electric field is 0.49 kV/mm. The corona ring shields the insulator from serious harm by converting the uneven electric field distribution into a uniform electric field distribution.

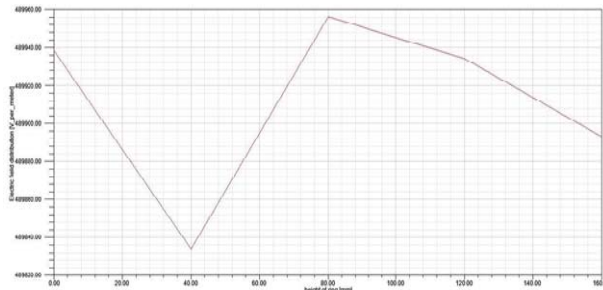


Fig 12. Diameter -700 m

At that moment, we fixed the diameter of ring at 700mm. When compared to 600mm there is reduced electric field distribution in 700mm ring. In 700mm ring the reduced electric field is achieved in 120mm height at high voltage side. At height of 120mm, the electric field distribution is 0.4kv/mm. At 80 mm in height, the maximum electric field is 0.49 kV/mm. It is shown in In Figure.12,

Electric field distribution in elliptical structure

The distribution of the electric field along the insulator is decreased by using a corona ring. Here, the ring's shape is altered to improve its effectiveness. So here elliptical ring structure is used. Figure.13.shows electric field distribution for various diameter of elliptical ring. The 400 mm diameter in this graph represents the highest electric field. When the ring diameter increased then electric field distribution also get reduced.

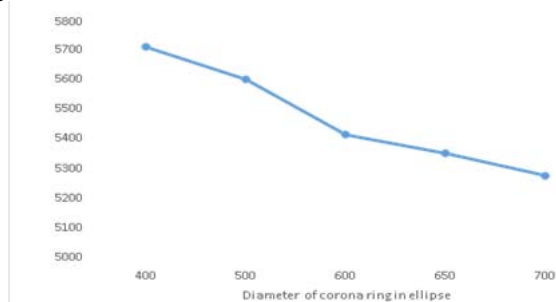


Fig. 13. Electrical field in ellipse structure

Minimum electric field distribution is achieved in the diameter of 700mm. Optimised value of diameter is 680mm. When compare to circular corona ring the elliptical structure reduces electric field distribution more.

We have used ring ratio of 0.5, inner diameter 80mm and the outer diameter of 680mm. The electric field distribution is 0.40kv/mm at dry condition. The most efficient corona ring shape is elliptical structure only. Figure.14.shows the Electric field distribution of ellipse shape corona ring

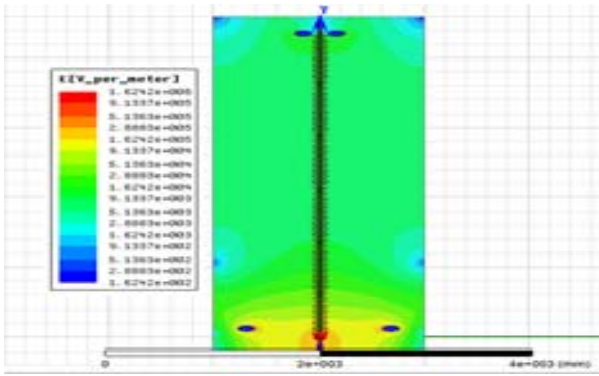


Fig 14. E field distribution of ellipse shape corona ring

When compare to circular corona ring the elliptical structure reduces electric field distribution more. We have an 80 mm inner diameter, a 680 mm outer diameter, and a ring ratio of 0.5. The electric field distribution is 0.43kv/mm at dry condition. The most efficient corona ring shape is elliptical structure only. Figure: 15. Ellipse ratio 0.5 at dry condition Figure: 16. Shows the Ellipse ratio 0.5 at wet condition

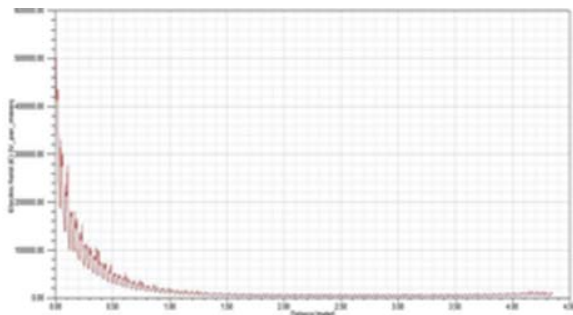


Fig: 15. Ellipse ratio 0.5 at dry condition

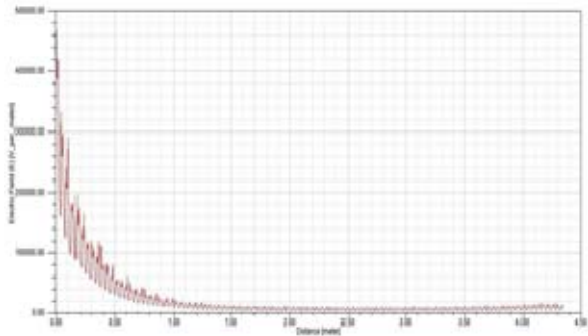


Fig: 16. Ellipse ratio 0.5 at wet condition

When compare to circular corona ring the elliptical structure reduces electric field distribution more. We have an 80 mm inner diameter, a 680 mm outer diameter, and a ring ratio of 0.5. The electric field distribution is 0.43kv/mm at dry condition. The most efficient corona ring shape is elliptical structure only. Figure: 15. Ellipse ratio 0.5 at dry condition Figure: 16. Shows the Ellipse ratio 0.5 at wet condition

Electric field distribution during polluted condition

Figure: 17 shows the insulator with elliptical ring at two ends at polluted condition by using sand as polluted material. The elliptical shape has a greater effect on minimizing the spread of the electric field than the circular shape. The distribution of the electric field in a contaminated state is shown in Figure. 18. Under these

circumstances, the wet condition electric field distribution is 0.42 kV/mm.

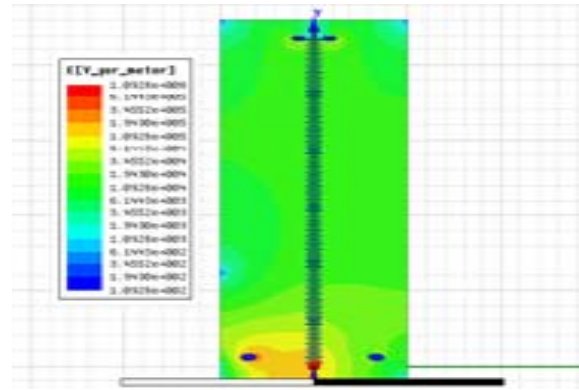


Fig: 17. Ellipse ring during polluted condition

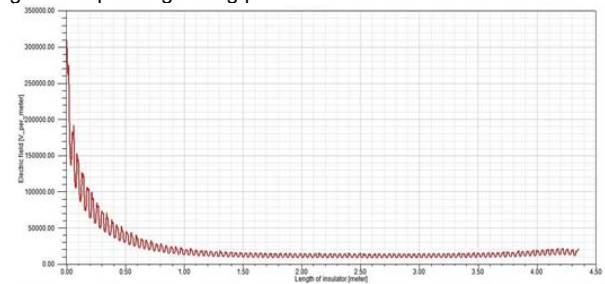


Fig. 18. Elliptical ring during polluted condition

The electric field distribution in a contaminated state is displayed in Figure. 19. In this condition the electric field distribution is 0.31kv/mm at dry condition.

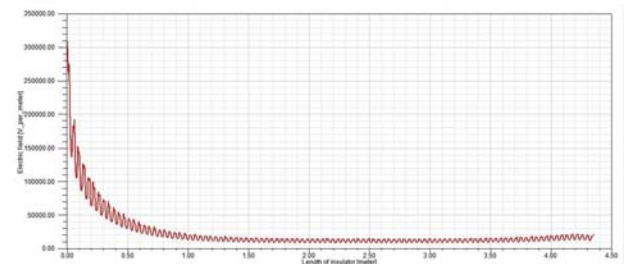


Fig. 19. Elliptical ring at dry and polluted condition

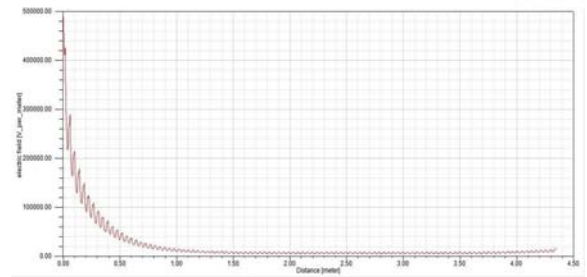


Fig: 20 Circular ring at polluted condition

When compare to wet condition there less electric field distribution in dry condition. Figure. 20 shows the circular ring at polluted condition

Electric field distribution in presence of water droplets

Due to climatic changes insulator will subjected to covered by rain water and ice. The electric field distribution in the water droplet state is higher than in the dry condition. Those water droplets act as conductive medium to increase the electric field distribution.

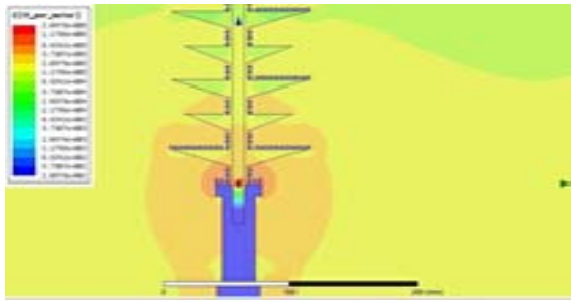


Fig.21 water droplets

The electric field distribution over the insulator with water droplets present but without a corona ring is shown in Figure. 21. The electric field distribution along the insulator with water droplets present but without a corona ring is shown in Figure. 22. Both the cases damage the insulator.

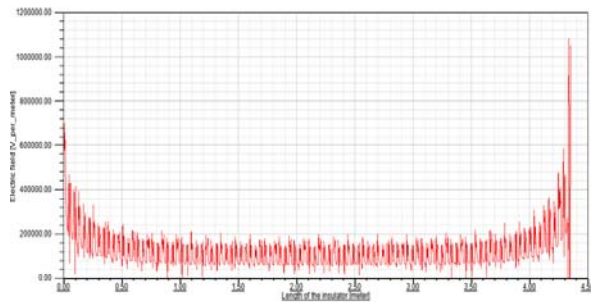


Fig.22. Electric field distribution

Structural analysis

Figure.23 shows the deformation of insulator. When we apply the force of 160KN from Table.3 at any one end of the insulator maximum deformation is observed in the triple junction which leads to complete damage of the insulator.

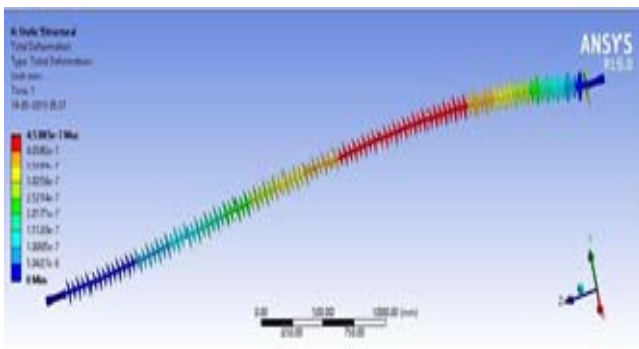


Fig. 23. Deformation of insulator

Stress analysis

Figure.24 shows the insulator subjected to stress. When we apply the force of 160KN according to the Table.3. At any one end of the insulator maximum stress is observed in the triple junction which leads to complete damage of the insulator.

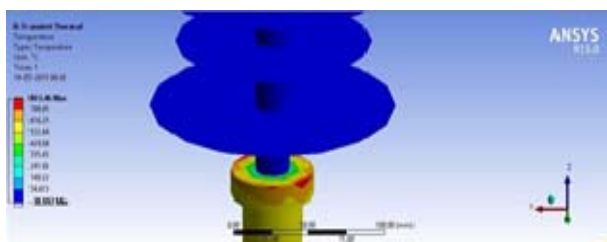


Fig. 24 The insulator subjected to stress.

Thermal analysis

Figure.25 shows the insulator subjected to thermal analyse. When we apply the temperature of 27°C (Environment temperature) to overall structure of the insulator maximum temperature observed in the triple junction is 803.46°C which leads to complete damage of the insulator.

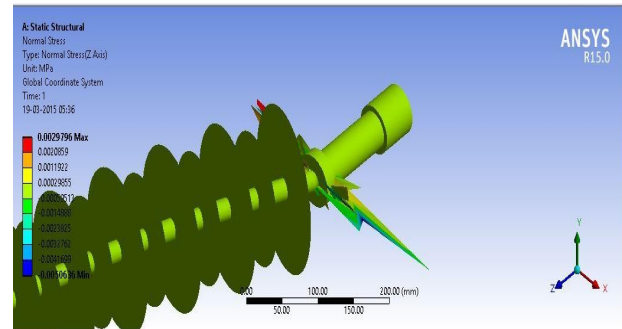


Fig. 25. The insulator subjected to thermal analysis

In the proposed algorithm, it is chosen that Population size=300, SA Cooling rate=0.95, Crossover rate = 0.7, Initial Temperature=1000°C, Mutation rate=0.001, Maximum iteration=1000, Roulette wheel selection, Single point crossover have utilized for the proposed method. From the analysis, it is recommended to use the large grading ring, which has dimensions of approximately 120 mm in height, 680 mm in diameter, and 80 mm in calibre. Alternatively, a small grading ring, measuring 00 mm in height, 150 mm in diameter, and 80 mm in calibre, can be used. By using ANSYS we have done structural analysis, thermal analysis and stress analysis.

In stress analysis we applied force of 160KN to check the deformation at triple point and in thermal analyse we applied temperature of 27°C (environment temperature) to check maximum withstanding temperature of the insulator.

Figure: 26. shows the convergence characteristics of Electric field distribution. After 20 iterations, the minimum goal function is reached. To verify the effectiveness and dependability of the optimization technique employed as well as the precision of the outcomes, the proposed optimization algorithm is compared with BAT, PSO, GA, SA, BPSO and IBPSO algorithms.

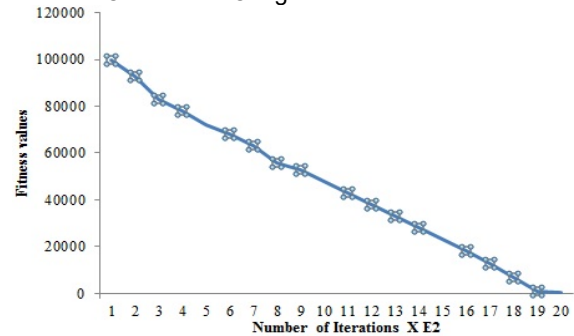


Fig: 26. Convergence characteristics of Electric field distribution

Table 4. Optimization Grading ring parameters

Parameters/Algorithm	H(mm)	R(mm)	T(mm)	E(Kv cm ⁻¹)
BAT[8]	310	200	80	1.87
PSO	325	200	88	1.91
GA	341	203	86	1.96
SA	305	206	85	1.84
BPSO	306	194	87	1.89
CSAIBPSO	302	188	78	1.78

Table 4 displays the acquired results. These findings show that the CSAIBPSO, BPSO, PSO, and GA approaches nearly produce the same outcomes. When compared to other approaches, the E-Field value optimized

by the CSAIBPSO algorithm matches to the minimum value, indicating that the process yields more accurate results. Obtaining the smallest value is our aim. In addition, From the Table 4 it is observed that that the CSAIBPSO method produces optimal electrical field distribution than other compared techniques.

Conclusion

In this paper, the FEM and CSAIBPSO approach is utilized to compute the potential and E-Field distribution. Without grading rings, the insulator's E-Field distribution is incredibly uneven, and some areas have maximal E-Field intensities that are higher than the corona inception value, which could lead to corona discharge. The conductor side of composite insulators shaped like circles experiences a larger electric field in a 765 kV than those shaped like ellipses. Quality solution is obtained by combining Very fast GA and IBPSO, Solution escapes from entapping from local minima. Therefore, elliptical shapes are more effective than circular ones at maintaining a uniform electric field distribution for insulator dependability. The optimization of grading ring geometrical parameters is done through CSAIBPSO improve its distribution.

Authors:

Dr.K.Suresh, Dr.K.Porkumaran, Dr.SanjeeviGandhi.A, Dr.G.Venkatesan, Mr.C.Jeeva, Department of Electrical and Electronics Engineering, Sri Sai Ram Engineering College, Chennai, India. Email:suresh.kaliyamoorthy@gmail.com

REFERENCES

- [1] R. S. Gorur, E. A. Cherney, and R. Hackam, "Polymer Insulator Profiles Evaluated In a Fog Chamber", *IEEE Transactions on Power Delivery*, Vol. 5, No. 2, pp. 1078–1085, April 1990.
- [2] R. Hartings, "Modern Experimental Techniques to Study the Discharge Phenomena on Outdoor Insulators", *Proceedings of the Seventh International Symposium on HV Engineering*, Dresden, Vol.1, August 1991.
- [3] S. Chakravorti, and P. K. Mukherjee, "Power Frequency and Impulse Field Calculation around a HV Insulator with Uniform or Non-uniform Surface Pollution", *IEEE Transactions on Dielectrics and Electrical Insulation*, Vol. 28, No.1, pp. 43-53, February 1993.
- [4] G. H. Vaillancourt, S. Carignan, and C. Jean, "Experience with the Detection of Faulty Composite Insulators on High-Voltage Power Lines by the Electric Field Measurement Method", *IEEE Transactions on Power Delivery*, Vol. 13, No. 2, pp. 661-666, April 1998.
- [5] Y. Chen, C. Li, X. Liang, and S. Wang, "The Influence of Water and Pollution on Diagnosing Defective Composite Insulators by Electric Field Mapping", *Proceedings of the Eleventh International Symposium on HV Engineering*, London, Vol. 3, pp. 197-200, August 1999.
- [6] G. Gela, and D. Mitchell, "Assessing the Electrical and Mechanical Integrity of Composite Insulators Prior to Live Working", *Proceedings of IEEE 9th International Conference on Transmission and Distribution Construction, Operation and Live-Line Maintenance*, Vol. 1, pp. 339–343, 2000.
- [7] Feng Huo, Peng Zhang, Yiliang Yu, Qin Liu, Lei Chu, Xuezhong Wang "Electric field calculation and grading ring design for 750kV four-circuits transmission line on the same tower with six cross-arms", *Journal of Engineering*, John Wiley, Vol. 1, No.16, pp. 3155-3159, 2019.
- [8] Nadjim Alti Abdelhafid, Bayadi Khaled, Belhouchet, "Grading ring parameters optimization for 220 kV metal-oxide arrester using 3D-FEM method and bat algorithm", *IET Science, Measurement & Technology*, Vol.15, pp.14-24, 2021-37, 2020.
- [9] Benalia m'hamdi, youcef benmahamed, Madjid teguar ,Ibrahim B.M.Taha , Sherif S. M. Ghoneim, "Multi-Objective Optimization of 400 kV Composite Insulator Corona Ring Design", *IEEE Access*, Vol.10, pp.27579-27590, 2022.
- [10] Shiling Zhang "Optimization of Corona Ring Design Used in UHV Composite Insulator by PSO Algorithm", *Journal of Physics*: Vol.1, pp1-10, 2021.
- [11] B. M'hamdi, M. Teguar and A. Mekhaldi, "Optimal Design of Corona Ring on HV Composite Insulator Using PSO Approach with Dynamic Population Size", *IEEE Transactions on Dielectrics and Electrical Insulation* ,Vol. 23, No. 2, 1048-1057, 2016.
- [12] J.S.T. Looms, "Insulators for High Voltage", Peter Peregrinus Ltd, London, U. K., 1988.
- [13] S. Chakravorti, and H. Steinbigler, "Boundary-Element Studies on Insulator Shape and Electric Field around HV Insulators with or without Pollution", *IEEE Transactions on Dielectrics and Electrical Insulation*, Vol. 7, No. 2, pp. 169-176, April 2000.
- [14] S.K.B.Pradeep Kumar Ch, G. Balamurugan, Y. Butchi raju "Optimal Infusion and Grading of Combined DGs and Capacitor Banks for Line Loss Minimization and Enhancement of Voltages in Radial Circuit System". *PRZEGLĄD ELEKTROTECHNICZNY*, ISSN 0033-2097, R. 97 NR 12/2021, pp.14-22, 2021.
- [15] T. Zhao, and M. G. Comber, "Calculation of Electric Field and Potential Distribution along Non-Ceramic Insulators Considering the Effects of Conductors and Transmission Towers", *IEEE Transactions on Power Delivery*, Vol. 15, No. 1, pp. 313-318, January 2000.
- [16] E. A. Cherney, "Non-Ceramic Insulators - a Simple Design that Requires Careful Analysis", *IEEE Electrical Insulation Magazine*, Vol. 12, No. 3, pp. 7-15, May/June 1996.
- [17] H.El-Kishky, and R. S. Gorur, "Electric Field and Energy Computation on Wet Insulating Surfaces", *IEEE Transactions on Dielectrics and Electrical Insulation*, Vol. 3, No. 4, pp. 587-593, August 1996.
- [18] G. H. Vaillancourt, S. Carignan, and C. Jean, "Experience with the Detection of Faulty Composite Insulators on High-Voltage Power Lines by the Electric Field Measurement Method", *IEEE Transactions on Power Delivery*, Vol.13, No.2, pp. 661-666, April 1998.
- [19] G. Gela, and D. Mitchell, "Assessing the Electrical and Mechanical Integrity of Composite Insulators Prior to Live Working," *Proceedings of IEEE 9th International Conference on Transmission and Distribution Construction, Operation and Live-Line Maintenance*, Montreal, Canada, Vol.1, pp.339–343, 2000.
- [20] G. H. Vaillancourt, J. P. Bellerive, M. St-Jean, and C. Jean, "New Live Line Tester for Porcelain Suspension Insulators on High-Voltage Power Lines", *IEEE Transactions on Power Delivery*, Vol. 9, pp. 208-219, January 1994,
- [21] Mohammad-Taghi, Vakil-Baghmisheh, Alireza NavarbaF "A modified very fast simulated annealing algorithm", *Proc IEEE Int Symposium on Telecommunications*. St. Petersburg, Russia, Vol.1, pp.61–66. 16–19, June 2008.
- [22] K.Suresh, N.Kumarappan "Hybrid improved binary particle swarm optimization approach for generation maintenance scheduling problem", *Elsevier-Swarm and Evolutionary Computation*, vol.9, pp.69-89, 2013.
- [23] Rong-Ceng Leou. "A new method for unit maintenance scheduling considering reliability and operation expense", *Elsevier-International Journal of Electrical Power & Energy Systems*, Vol.28, No.7, pp.471-481, 2006.
- [24] E.Kufel, W. S. Zaengel, "High Voltage Engineering Fundamentals", Pergamon Press, 1988.
- [25] Benalia M'hamdi, Youcef Benmahamed, Madjid Teguar Ibrahim B. M. Taha, Sherif S. M. Ghoneim, "Multi- Objective Optimization of 400 kV Composite Insulator Corona Ring Design", *IEEE Access*, Vol.10, pp.27579–27590, March 8, 2022.